ELSEVIER

Journal of Alloys and Compounds 408–412 (2006) 1071–1077

Journal of ALLOYS AND COMPOUNDS

www.elsevier.com/locate/jallcom

$LaFePdO_3$ perovskite automotive catalyst having a self-regenerative function

Hirohisa Tanaka [a,*], Isao Tan [a], Mari Uenishi [a], Masashi Taniguchi [a], Mareo Kimura [b], Yasuo Nishihata [c], Jun'ichiro Mizuki [c]

[a] *Materials Research and Development Division, Daihatsu Motor Co., Ltd., Osaka 563-8651, Japan*
[b] *Research and Development Division, Cataler Corporation, Shizuoka 437-1492, Japan*
[c] *Synchrotron Radiation Research Center, Japan Atomic Energy Research Institute, Hyogo 679-5148, Japan*

Received 30 July 2004; received in revised form 15 December 2004; accepted 15 December 2004
Available online 13 June 2005

Abstract

An automotive gasoline engine is operated close to the stoichiometric air-to-fuel ratio to convert the pollutant emissions simultaneously, accompanying with redox (reduction and oxidation) fluctuations in exhaust-gas composition through adjusting the air-to-fuel ratio. An innovative $LaFe_{0.95}Pd_{0.05}O_3$ perovskite catalyst, named 'the intelligent catalyst', has been developed, and which has a new self-regenerative function of the precious metal in the inherent fluctuations of automotive exhaust-gas.

The $LaFe_{0.95}Pd_{0.05}O_3$ perovskite catalyst, La located at the A-site, was prepared by the alkoxide method. Pd located at the B-site of the perovskite lattice in the oxidative atmosphere, and segregated out to form small metallic particles in the reductive atmosphere. The catalyst retained a predominantly perovskite structure throughout a redox cycle of the exhaust-gas, while the local structure around Pd could be changed in a completely reversible manner. The agglomeration and growth of Pd particles is suppressed, even under the severe environment, as a result of the movement between inside and outside the perovskite lattice. It is revealed that the self-regenerative function of Pd occurs even at 200 °C, unexpectedly low temperature, in the $LaFe_{0.95}Pd_{0.05}O_3$ catalyst. Since the high catalytic activity is maintained, the great reduction of Pd loading has been achieved. The intelligent catalyst is expected as a new application of the rare earth, and then the technology is expected in the same way in the global standard of the catalyst designing.

Keywords: Perovskite; Palladium; Regeneration; Super ultra low emission vehicle

1. Introduction

1.1. Background

Rare earth oxides have widely been applied to the automotive catalyst. Ceria, having an excellent oxygen storage capacity, is the most popular rare earth oxide in the three-way catalyst. And La and Nd are doped into alumina, zirconia and ceria to improve their thermal stabilities. A quite new application of rare earth was shown in the present paper: a $LaFe_{0.95}Pd_{0.05}O_3$ perovskite catalyst, named 'the intelligent catalyst', which has a self-regenerative function of precious metals in the inherent fluctuations of automotive exhaust-gas [1–6].

Emission regulations are getting tighter and tighter, in order to guarantee cleaner air for the environment, all over the world. The Japanese government has introduced cleaner emission standards designated as ULEV and super ultra low emission vehicle (SULEV), which are in order, 50 and 75% reductions of HC and NO_x in comparison with standards for emission regulation set in the year 2005.

The increasing amounts of precious metals must be required to meet these severe regulations when traditional catalyst technologies are applied. Demand for Pd for use in automotive catalysts, in particular, has burgeoned from 15 to

* Corresponding author. Tel.: +81 72 754 3205; fax: +81 72 754 3444.
E-mail address: hirohisa_tanaka@mail.daihatsu.co.jp (H. Tanaka).

0925-8388/$ – see front matter © 2005 Elsevier B.V. All rights reserved.
doi:10.1016/j.jallcom.2004.12.138

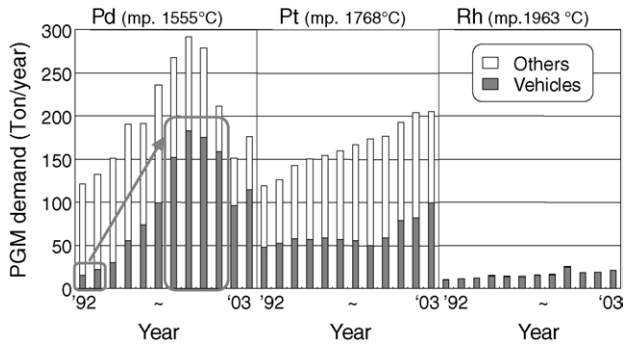

Fig. 1. Annual demand for PGMs.

150 tonnes per year over the last decade (Fig. 1) [7]. This drastic increase is due to the strengthening of the worldwide cold emission regulations, which has made development of the reduction technologies so urgent.

The intelligent catalyst with the function for self-regeneration of Pd, through the solid solution and segregation of Pd in the perovskite crystal, succeeds in utilization and is supplied to the market from 2002. The Japan super ultra low emission vehicle standard has been achieved with mounting a single intelligent catalyst at the manifold, right under the engine position. The intelligent catalyst is expected as the solution that can reduce the use of precious metals, especially Pd.

1.2. History of perovskite catalyst

A perovskite-type oxide has an ABO_3-type crystal structure wherein cations with a large ionic radius have 12 coordination to oxygen atom and occupy A-sites, and cations with a smaller ionic radius have 6 coordination and occupy B-sites. A and O form a cubic closest packing, and B is contained in the octahedral voids in the packing. If the ionic radii are r_A, r_B and r_O, to form a perovskite crystal structure, the tolerance factor $(t) = (r_A + r_O)/\sqrt{2}(r_B + r_O)$ must lie within the range $0.8 < t < 1.0$, and $r_A > 0.090$ nm, $r_B > 0.051$ nm. A great many elements can form ideal or modified perovskites depending on the tolerance factor.

Perovskite-type compounds, especially which contain rare earth metals at A-site, are interesting materials for catalytic applications and for fundamental studies as well. Many studies on perovskite catalysts have been reported [8–23].

The characteristics of perovskite catalysts are summarized as below:

(1) In $LnMO_3$ (Ln = lanthanoid, M = transition metals) perovskites, the catalytic activity for oxidation is mainly determined by B-site elements, in the order Co > Mn > Ni > Fe > Cr.
(2) In $LnMO_3$ perovskites, the structual stability in a reductive atmosphere is also determined by B-site elements, in the order Cr > Fe > Mn > Co > Ni.
(3) One of the advantages of the formation of a perovskite structure is to increase the thermal stability of the transition metal oxides.
(4) Another advantage is the valency and vacancy control to enhance their catalytic activity.

It was also reported that Pd containing $LaCeFeCoO_3$ showed the excellent three-way catalytic activity for automotive emissions control [24,25]. But it is required to remove cobalt (Co), which has been singled out by TA-luft as a carcinogenic, for the industrialization of the perovskite catalyst as the practical intelligent catalyst [5,6,26].

In this paper, the self-regenerative function and its temperature dependency of Co-free perovskite, $LaFe_{0.95}Pd_{0.05}O_3$, were investigated.

2. Experimental

2.1. Preparation of catalyst

2.1.1. Powder catalyst

A Pd-containing $LaFe_{0.95}Pd_{0.05}O_3$ perovskite powder catalyst was prepared by the alkoxide method [2]. Metal ethoxyethylates, M^{3+} $(OC_2H_4OC_2H_5)_3$, of La, Fe were dissolved in toluene, a precipitate containing Pd was obtained by using a diluted palladium nitrate aqueous solution during hydrolysis, and after drying, the precursor was calcined at 700 °C for 4 h in air to obtain a perovskite powder catalyst containing Pd homogeneously. A Pd/Al_2O_3 powder catalyst was prepared as a reference. Al_2O_3 was impregnated with palladium nitrate solution, then dried and calcined in an air furnace at 700 °C for 4 h.

2.1.2. Monolithic catalyst

Each powder catalyst was coated on the inner wall of a monolithic honeycomb substrate (80 mm in diameter and 95 mm in length with the grid of 64 cell cm^{-2}), containing the same amount of Pd (3.24 mg cm^{-3}). Table 1 summarizes the configuration of the monolithic catalysts for fundamental research.

2.2. Thermal treatment and engine aging

2.2.1. Redox treatment for powder catalyst

To begin with, the possibility of self-regenerative function of Co-free perovskite, $LaFe_{0.95}Pd_{0.05}O_3$, and its temperature dependency were investigated. Thermal treatment was carried out in three steps to simulate the redox fluctuations of an automotive exhaust-gas.

Table 1
Monolithic catalyst configuration

Composition	Pd (mg cm^{-3})
$LaFe_{0.95}Pd_{0.05}O_3$	3.24
Pd/Al_2O_3	3.24

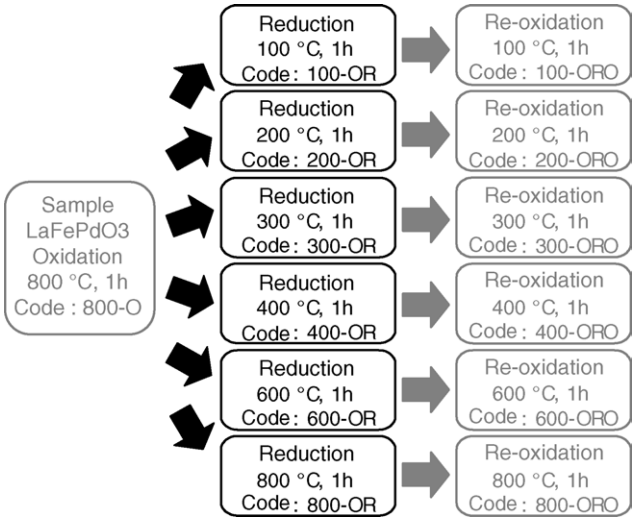

Fig. 2. Redox treatment procedure [27,28].

First, the catalyst was oxidized in an air at 800 °C for 1 h. Then, the sample was reduced in 2.5% H_2 and 7.5% CO balanced with N_2 for 1 h at 100, 200, 300, 400, 600 and 800 °C, respectively. Finally, the sample was re-oxidized in air for 1 h at the same temperatures as reductive treatment (Fig. 2).

This successive single-run treatment creates a separate model for each of the key stages of the engine exhaust atmosphere's evolution [4,27,28].

2.2.2. Aging of monolithic catalyst in engine exhaust at 900 °C

Next, self-regenerative function of the catalyst in the actual engine exhaust was investigated. The monolithic catalysts, for research, were aged at 900 °C (catalyst inlet temperature) for 100 h in exhaust-gas from a real 4000 cm^3 V-8 engine. The fuel for aging was regular grade gasoline that contained approximately 50 ppm of sulphur. During exposure, two exhaust-gas conditions were alternated: an atmosphere with large air-to-fuel ratio fluctuations ($\Delta\lambda = \pm 4\%$ at 0.6 Hz) around the stoichiometric point was applied for 870 s, then an oxidizing atmosphere for 30 s. The total engine aging time is the sum of 400 cycles. This aging procedure is widely accepted for the simulation of a driving strategy to achieve higher fuel economy by introducing fuel cut-off during deceleration [29,30].

2.3. Characterization

2.3.1. X-ray analysis for $LaFePdO_3$ powder catalyst

The crystal structure of $LaFe_{0.95}Pd_{0.05}O_3$ powder catalyst after redox treatments at 800 °C was measured by X-ray diffraction (XRD) using Cu Kα [5].

The binding energy of Pd after redox treatments at 800 °C was analyzed using Mg Kα in X-ray photoelectron spectroscopy (XPS). The powder of PdO and Pd were measured as the standard materials [5].

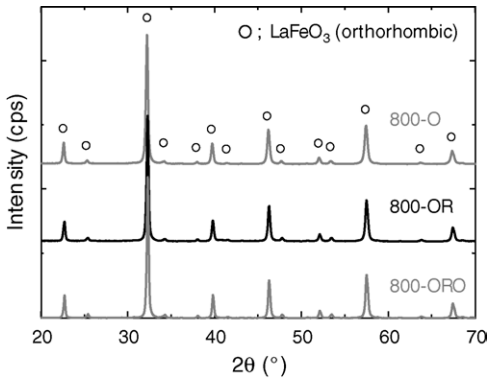

Fig. 3. XRD of $LaFe_{0.95}Pd_{0.05}O_3$ after redox treatments at 800 °C.

X-ray absorption fine structure (XAFS) was measured at bending-magnet beam lines at BL01B1 and BL14B1 in SPring-8. The spectra were measured near the Pd K-edge in transmission mode because of the high transmissivity of the X-ray. The Pd-foil and the powder of PdO were also measured as the standard materials, and the photon energy was calibrated with the Pd-foil by assigning 24.350 keV to the energy at half the edge jump.

2.3.2. Pd particle observation after engine aging

Pd particles of the catalysts, after aging in engine exhaust-gas at 900 °C for 100 h and cooling down in a reductive atmosphere, were observed by transmission electron microscopy (TEM).

2.4. Evaluation of catalytic activity

2.4.1. Switching light-off

Switching light-off test is a method for measuring the activation response from the cold ambient. The hot gas at 470 °C was rapidly introduced into the catalyst retained at 25 °C [5]. The space velocity at the catalyst inlet was maintained at 100,000 h^{-1} and air-to-fuel ratio was set at stoichiometic point. By using this method, an accurate model of the catalytic performance of actual vehicles at cold start is created for evaluation.

3. Results and discussion

3.1. XRD and XPS analyses for $LaFePdO_3$ powder catalyst

Fig. 3 shows the result of XRD for the $LaFe_{0.95}Pd_{0.05}O_3$ powder catalysts after oxidation, reduction and re-oxidation treatments at 800 °C. The durable perovskite structure was confirmed after redox treatments.

The states of Pd on the surface of powder catalysts, after oxidation, reduction and re-oxidation treatments at 800 °C, were analyzed by XPS. The results are shown in Fig. 4.

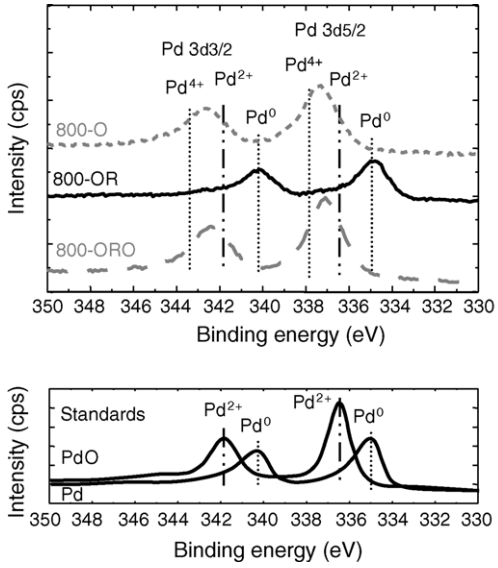

Fig. 4. XPS spectra of Pd for $LaFePdO_3$ after redox treatments at 800 °C.

Binding energies were corrected based on measured values for C 1s. The values for Pd^0 and binding energy of Pd in oxidized $LaFe_{0.95}Pd_{0.05}O_3$ perovskite indicates an extraordinary high oxidized state of Pd^{3+} or Pd^{4+}, the same as was previously reported [2]. The Pd in the reduced sample was found to be in metallic state. In the re-oxidized sample, the state of Pd was once again estimated at Pd^{3+} or Pd^{4+}. Pd^{2+} were determined in the comparison with metallic Pd and PdO, respectively.

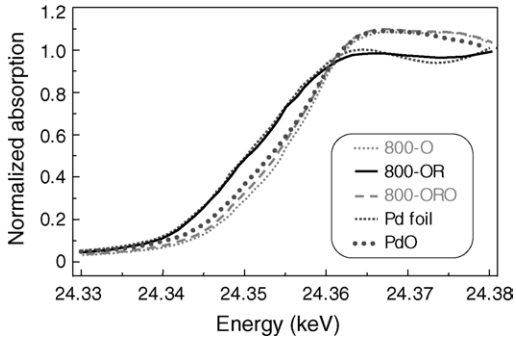

Fig. 5. XANES at Pd K-edge.

3.2. XAFS analysis for $LaFePdO_3$ powder catalyst

Fig. 5 shows X-ray absorption near edge structure (XANES) spectra at the Pd K-edge for $LaFe_{0.95}Pd_{0.05}O_3$ perovskite, after oxidation, reduction and re-oxidation treatments at 800 °C, together with the XANES spectra of Pd-foil and Pd–O as the standard materials [31].

After oxidation treatment, the chemical shift observed at the edge position indicates, equal to the XPS analysis that

Table 2
Local structure parameters of $LaFe_{0.95}Pd_{0.05}O_3$ treated at 800 °C estimated by EXAFS [31]

K-edge	Ageing treatment	Shell (bond)	Weight (W_{shell})	Coordination number	Interatomic distance (nm)	Debye–Waller factor ($\times 10^{-4}$ nm^2)	Discrepancy factor (%)
Pd	800-O	Pd–O	1	6*	0.2038(5)	0.58(3)	3.9
	800-OR	Pd–Pd/Pd–Fe	0.44	6*/6*	0.2683(3)	0.64(4)	8.6
		Pd–Pd	0.20	12*	0.2743(1)	0.64†	
	800-ORO	Pd–O	1	6*	0.2038(5)	0.65(3)	8.9

The value marked with "*" was fixed parameter, and with "†" was treated as the same value for the other shell.

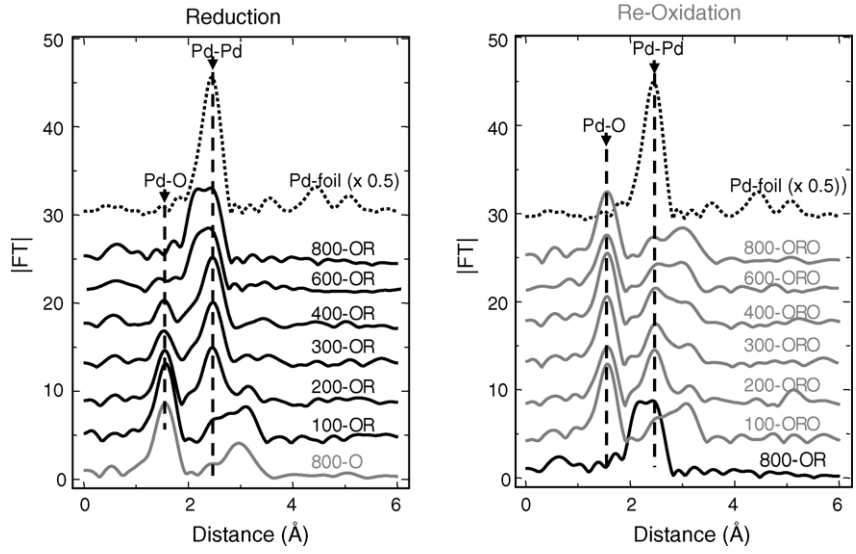

Fig. 6. Radial structure function around Pd.

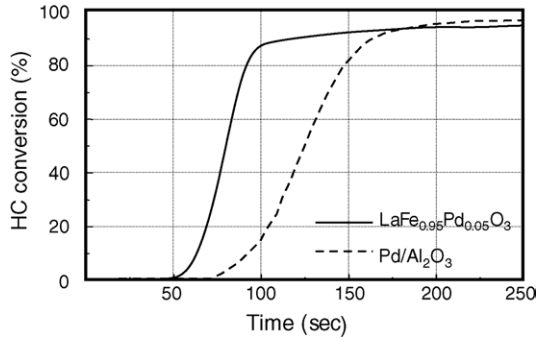

Fig. 7. Switching light-off performance.

Pd in $LaFe_{0.95}Pd_{0.05}O_3$ perovskite is in a 3+ or 4+ state. The edge position of the reduced catalyst, on the other hand, is identical to that of Pd-foil, suggesting that Pd is in a metallic state. Finally, after re-oxidation treatment, the edge position shifted back to higher energy.

The radial structure function around Pd was obtained by Fourier transform of extended X-ray absorption fine structure (EXAFS) oscillations (Fig. 6). The local structure parameters of the first nearest neighbor around the Pd in $LaFe_{0.95}Pd_{0.05}O_3$ after redox treatments at 800 °C, obtained by a standard EXAFS analysis according to Mckale et al., was shown in Table 2.

At first Pd of the sample oxidized at 800 °C (800-O), occupies the B-site, in the six-fold coordination with oxygen, of the unit formula of ABO_3 in a perovskite structure.

When the sample was reduced and Pd was segregated from perovskite crystal to form small metallic particles, the first nearest peak height corresponding to the Pd–O bond got lower, and the second peak corresponding to the Pd–Pd bond got higher as the reduction temperature increased from 200 °C. At 800 °C, the peak shows the mixture of Pd–Pd and Pd–Fe bonds (800-OR). Note that the summation of the weight both of Pd–Pd and Pd–Fe is only 0.64, it means the deposited metal particle is very small.

In a re-oxidative atmosphere, the amount of the Pd–Pd bond decreased from 200 °C (Fig. 6). After re-oxidation at 800 °C (800-ORO), the Pd–Pd bond disappeared, and the local structure around Pd is completely the same as that of the oxidized catalyst (800-O).

The results of XAFS analysis indicates that Pd of Co-free $LaFe_{0.95}Pd_{0.05}O_3$ perovskite moves in a completely reversible manner in subsequent redox fluctuations. The agglomeration and growth of the metal particles is suppressed as a result of the structural change due to the inherent fluctuation between reductive and oxidative (redox) atmospheres in automotive exhaust from common gasoline engines. Also, it is revealed that this regenerative function of Pd occurred from unexpectedly low temperatures.

3.3. Catalytic activity in switching light-off

The results of switching light-off performances of the monolithic catalysts after aging in engine exhaust-gas at 900 °C for 100 h were shown in Fig. 7. $LaFe_{0.95}Pd_{0.05}O_3$ showed excellent ability to reduce HC emissions during cold starting. Note that the amount of precious metals was set to be equivalent for each catalyst. It would be assumed that the moving of Pd from very low temperatures gave the good effect for light-off performance.

3.4. Pd particle observation after engine aging

TEM observations of Pd particles of the monolithic catalysts, after aging in engine exhaust-gas at 900 °C for 100 h and cooling down in a reductive atmosphere, were shown in Fig. 8. The magnification for $LaFe_{0.95}Pd_{0.05}O_3$ is 400,000 times and the white bar shows 10 nm, and the magnification for Pd/Al_2O_3 is 100,000 times and the white bar shows 50 nm.

Pd metallic particles of $LaFe_{0.95}Pd_{0.05}O_3$ maintained finer grain size by about 1 nm in diameter. From EXAFS, the average particle size of Pd particle is also estimated to be about 1.1 nm [32].

However, the particle of Pd on Al_2O_3 enlarged up to 120 nm, and the average particle diameter by CO chemisorption was 32 nm, and the crystallite size measured at Pd(1 1 1) by XRD was 58 nm.

It is confirmed that $LaFe_{0.95}Pd_{0.05}O_3$ has an excellent ability to suppress the grain growth of Pd. Pd keeps its atomic

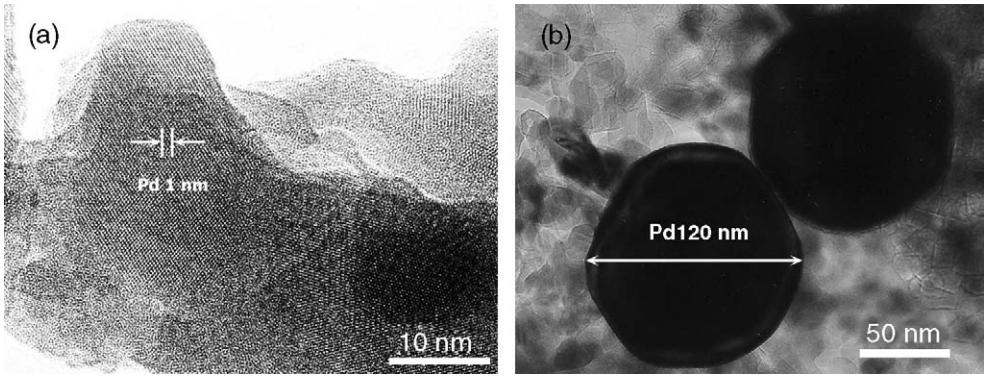

Fig. 8. TEM observation of Pd on catalysts after engine aging at 900 °C: (a) $LaFe_{0.95}Pd_{0.05}O_3$ and (b) Pd/Al_2O_3.

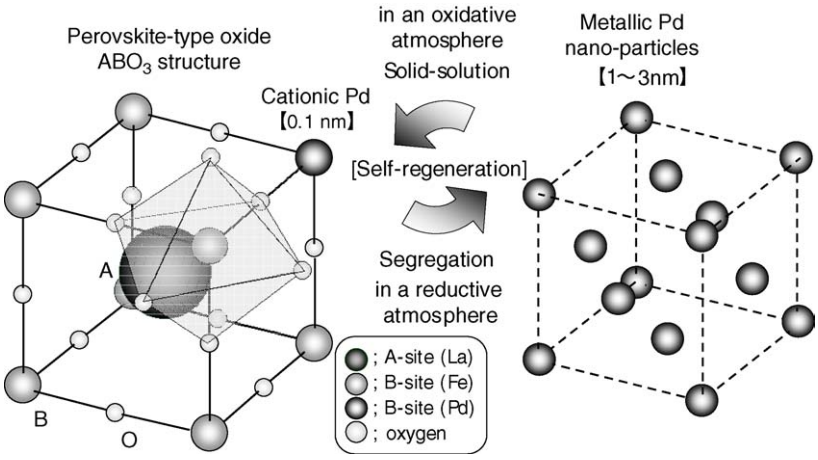

Fig. 9. Self-regenerative function of the intelligent catalyst [26].

size by moving in and out of the crystal according to the characteristic fluctuation of redox atmospheres in automotive exhaust-gas.

3.5. Self-regenerative function of $LaFePdO_3$

It was reported that a $LaFe_{0.57}Co_{0.38}Pd_{0.05}O_3$ perovskite catalyst has the function of self-regeneration of Pd in the previous paper [3]. In this paper, it is confirmed that Pd in a Co-free $LaFe_{0.95}Pd_{0.05}O_3$ catalyst also moves back and forth between the B-site in the perovskite structure and the metallic particle, when exposed to inherent fluctuations of the actual engine exhaust. Fig. 9 shows a graphic illustration of the self-regenerative function that is the core technology, of the intelligent catalyst. This self-regenerative function of the intelligent catalyst can suppress the grain growth of Pd and can save amount of precious metals.

$LaFe_{0.95}Pd_{0.05}O_3$ perovskite catalyst has been industrialized for SULEV. The intelligent catalyst is expected as new catalyst design technology, which can solve the problem of the precious metal supply and demand.

4. Conclusion

1. From X-ray research, it has been proved that Pd in $LaFe_{0.95}Pd_{0.05}O_3$ reversibly moves back and forth between the B-site in the perovskite structure and the metal particle lattice.
2. It is revealed that the self-regenerative function of Pd in the $LaFe_{0.95}Pd_{0.05}O_3$ catalyst occurs from very low temperatures.
3. Self-regenerative function suppresses the grain growth of precious metals.
4. Light-off performance of the intelligent catalyst is much better than that of the contemporary catalyst due to the suppression of Pd grain growth.
5. Rare earth metal containing $LaFe_{0.95}Pd_{0.05}O_3$ perovskite catalyst has been industrialized for SULEV (super ultra low emission vehicle).
6. The intelligent catalyst is one solution for the Pd supply and demand problem.

Acknowledgements

The authors would like to thank Professor Emeritus Dr. M. Misono and Professor Dr. N. Mizuno of the University of Tokyo for their advice. Mr. K. Kaneko and Mr. S. Mitachi of Hokko Chemical Industry Co., Ltd., are gratefully acknowledged for their support in powder preparations. The authors would like to thank Mr. Y. Sato, Mr. K. Narita and Mr. N. Sato of Cataler Corp. for their support in industrialization. Mr. K. Mitsumori, Mr. I. Takahashi and Mr. N. Kajita of Daihatsu Motor Co., Ltd. are also acknowledged for their help.

The synchrotron radiation research was supported partly by The Ministry of Education, Culture, Sports, Science and Technology; KAKENHI (15350090), and was performed at the SPring-8 with the approval of the Japan Synchrotron Radiation Research Institute (JASRI).

References

[1] H. Tanaka, I. Takahashi, M. Kimura, H. Sobukawa, Science and Technology in Catalysis, Kodansha Elsevier, 1995, p. 457.
[2] H. Tanaka, I. Tan, M. Uenishi, M. Kimura, K. Dohmae, Topics in Catalysts, vols. 16–17, Kluwer Academic, New York, 2001, p. 63.
[3] H. Tanaka, M. Uenishi, I. Tan, M. Kimura, J. Mizuki, Y. Nishihata, SAE Paper No. 2001-01-1301, Society of Automotive Engineers, Pennsylvania, 2001.
[4] Y. Nishihata, J. Mizuki, T. Akao, H. Tanaka, M. Uenishi, M. Kimura, T. Okamoto, N. Hamada, Nature 418 (2002) 164.
[5] I. Tan, H. Tanaka, M. Uenishi, N. Kajita, M. Taniguchi, Y. Nishihata, J. Mizuki, SAE Paper No. 2003-01-0812, 2003.
[6] N. Sato, H. Tanaka, I. Tan, M. Uenishi, N. Kajita, M. Taniguchi, K. Narita, M. Kimura, SAE Paper No. 2003-01-0813, 2003.

[7] Platinum (Annual report) 2004 edition, Johnson Matthey.
[8] D.B. Meadowcroft, Nature 226 (1970) 847.
[9] G. Parravano, J. Chem. Phys. 20 (1952) 342.
[10] W.F. Libby, Science 171 (1971) 499.
[11] Y.F.Y. Yao, J. Catal. 36 (1975) 266.
[12] R.J.H. Voorhoeve, J.P. Remeika, L.E. Trimble, A.S. Cooper, F.J. Disalvo, P.K. Gallagher, J. Solid State Chem. 14 (1975) 395.
[13] T. Kudo, T. Gejo, K. Yoshida, Environ. Sci. Tech. 12 (1978) 185.
[14] T. Nakamura, G. Petzow, L.J. Gauckler, Mater. Res. Bull. 14 (1979) 649.
[15] H. Fujii, N. Mizuno, M. Misono, Chem. Lett. (1987) 2147.
[16] R.M. Hazen, Sci. Am. 6 (1988) 52.
[17] T. Nitadori, T. Ichiki, M. Misono, Bull. Chem. Soc. Jpn. 61 (1988) 621.
[18] K. Tabata, S. Kohiki, J. Mater. Sci. 23 (1988) 1056.
[19] L.G. Tejuca, J.L.G. Fierro, J.M.D. Tascon, Adv. Catal. 36 (1989) 237.
[20] L. Forni, C. Oliva, T. Barzetti, E. Selli, A.M. Ezerets, A.V. Vishniakov, Appl. Catal. B: Environ. 13 (1997) 35.
[21] Z. Shao, G. Xiong, S. Sheng, H. Chen, L. Li, Stud. Surf. Sci. Catal. 118 (1998) 431.
[22] V. Szabo, M. Bassir, J.E. Gallot, A.V. Neste, S. Kaliaguine, Appl. Catal. B: Environ. 42 (2003) 265.
[23] H. Tanaka, N. Mizuno, M. Misono, Appl. Catal. A: Gen. 244 (2003) 371.
[24] H. Tanaka, H. Fujikawa, I. Takahashi, SAE Paper No. 930251, 1993.
[25] H. Tanaka, H. Fujikawa, I. Takahashi, SAE Paper No. 950256, 1995.
[26] H. Tanaka, M. Taniguchi, N. Kajita, M. Uenishi, I. Tan, N. Sato, K. Narita, M. Kimura, Top. Catal. 30–31 (2004) 389.
[27] M. Uenishi, M. Taniguchi, H. Tanaka, M. Kimura, Y. Nishihata, J. Mizuki, T. Kobayashi, Appl. Catal. B: Environ. 57 (2005) 267.
[28] H. Tanaka, M. Uenishi, M. Taniguchi, M. Kimura, Y. Nishihata, J. Mizuki, Poster Session 6-119 ICC 13th, Paris, July 11–16, 2004.
[29] R.M. Heck, R.J. Farrauto, Catalytic Air Pollution Control: Commercial Technology, Van Nostrand Reinhold, New York, 1995.
[30] A. Waltner, G. Loose, A. Hirschmann, L. Muβmann, D. Lindner, W. Muller, SAE Paper No. 980663, 1998.
[31] Y. Nishihata, J. Mizuki, H. Tanaka, M. Uenishi, M. Kimura, J. Phys. Chem. Solid 66 (2005) 274.
[32] I. Tan, M. Taniguchi, H. Tanaka, M. Uenishi, N. Kajita, Y. Nishihata, J. Mizuki, K. Niihara, J. Ceram. Soc. Jpn., in press.